Nuclear Materials and Energy 16 (2018) 19–23

Contents lists available at ScienceDirect

Nuclear Materials and Energy

journal homepage: www.elsevier.com/locate/nme

# Evaluation of hardening behavior under synergistic interaction of He and subsequent H ions irradiation in vanadium alloys

S.N. Jiang[a,*], L.Q. Xu[a], P.F. Zheng[b]

[a] School of Mechanical & Automotive Engineering, Qilu University of Technology (Shandong Academy of Science), Jinan 250353, China
[b] Southwestern Institute of Physics, Chengdu 610041, China

ARTICLE INFO

*Keywords:*
Ion irradiation
Defect
Dislocation loop
Bubble
Irradiation hardening

ABSTRACT

Helium and hydrogen synergy effect on irradiation hardening in V-4Cr-4Ti alloys was investigated. The samples were irradiated helium or helium + hydrogen ions at RT (room temperature) and 300 °C. Transmission electron microscopy (TEM) and nano-indentation test were used to investigate the defects and hardness evolution induced by ion irradiation, respectively. The curves for irradiation induced hardness have been analyzed by indentation size effect (ISE) and soft substrate effect (SSE) on the basis of Nix-Gao model and Kasada's method. Point defects appeared after irradiation at RT and dislocation loops and bubbles observed after irradiation at 300 °C were responsible for hardening. The hardness after He + H ions irradiation at RT increased comparison with that of He irradiation samples at RT and 300 °C because the synergistic interaction of pre-implanted He, subsequent H and the irradiation-induced defects may affect the evolution of hardening. Bulk hardness could be evaluated by least square method. Besides ISE, SSE was observed in sample after irradiated He + H at 300 °C.

## 1. Introduction

Due to high temperature properties and low activation, vanadium-based alloys are considered as candidate structural materials for fusion reactor [1]. However, the presence of point defects (vacancies and interstitials), transmutation-created helium (He) and hydrogen (H) play important roles in microstructural evolution of V-4Cr-4Ti alloy under neutron irradiation which cause severe irradiation damage following the degradation of properties [2]. Helium combines with vacancy to form helium-vacancy clusters that promote the nucleation of He bubbles which cause irradiation hardening and embrittlement [3–5]. Defect clusters and dislocation loops also contribute to irradiation hardening. Jin *et al* irradiated Fe ions to Fe–Cr alloys and found dislocation loops as a strong obstacle for dislocation movement which brought about irradiation hardening [6]. However, the hardening caused by He ions implantation might result from two separate pinning centers: dislocation loops and bubbles [7–8]. Therefore, it is worth more investigation. In addition, the potential synergy effect of He and H on hardening needs further investigation under irradiation [9]. Study of hardening after H and He irradiation in V-4Ti found that defects or defects clusters during irradiation caused irradiation hardening for V-4Ti and pure V chiefly [10]. While other study found that dislocation loop instead of bubble induced irradiation hardening when irradiated H into He-pre-irradiated CLAM (China low activation ferritic martensitic steel) at 500 °C [11]. How H ion irradiation affects irradiation hardening in He pre-irradiated V-4Cr-4Ti alloy needs further confirmation.

As an effective simulation experiment, ion irradiation is often used to replace neutron irradiation for irradiation damage of materials. However, the small size and shallow projected range limit the use of conventional mechanical testing methods. Nanoindentaion measurement test has been successfully used to characterize the properties of thin ion implanted region recently [12]. Yang et al. studied the correlation between Vickers hardness and nano-hardness for the convenience of assessing mechanical properties of materials under irradiation and found a good linear relation between Vickers hardness and nano-hardness [13]. Based on this correlation, the data from ions irradiation was in good agreement with the data from neutron irradiation. Many correlated studies reported the hardness after ion irradiation tested using the continuous stiffness measurement (CSM) of nanoindentaion [14–15].

In this research, microstructure and mechanical property of V-4Cr-4Ti were studied after He and He + H ions irradiation at RT and 300 °C. Effect of H on He-implanted V-4Cr-4Ti alloy was studied. Microstructural evolution and resulting irradiation hardening were

* Corresponding author.
*E-mail address:* jsn@qlu.edu.cn (S.N. Jiang).

https://doi.org/10.1016/j.nme.2018.06.008
Received 28 November 2017; Received in revised form 5 June 2018; Accepted 8 June 2018

**Table 1**
The parameters of ion irradiation.

| Alloy number | 1 | 2 | | 3 | 4 | |
|---|---|---|---|---|---|---|
| Temperature (°C) | RT | RT | | 300 | 300 | |
| Ion | He | He | H | He | He | H |
| Energy (keV) | 80 | 80 | 50 | 80 | 80 | 50 |
| Fluence (ions.m$^{-2}$) | $1 \times 10^{21}$ | $1 \times 10^{21}$ | | $1 \times 10^{21}$ | $1 \times 10^{21}$ | |

discussed.

## 2. Experimental

### 2.1. The preparation of samples

The samples used in this study were V-4Cr-4Ti alloys (SWIP-30) from Southwestern Institute of Physics. They were solid soluted at 1373 K for 2 h and then prepared for TEM samples and nanoindentation samples. Size of TEM samples was Φ 3 mm × 100 µm and electron polished by twin-jet electropolisher. Nanoindentation samples were small pieces with the size of 10 mm × 10 mm × 2 mm after polishing.

### 2.2. Ion irradiation

Ion irradiation experiments were performed with an ion accelerator in Wuhan University with He ions and He + H ions. Ion energy and fluences for ion irradiation experiments are shown in Table 1. For convenience, four series of samples were numbered 1, 2, 3 and 4 which corresponded to He at RT, He + H at RT, He at 300 °C and He + H at 300 °C.

The damage induced by ion irradiation did not uniformly distribute in ion projected range which meant different damage and ion concentration for different depth. Fig. 1 shows irradiation damage profile and concentration of implanted ions calculated by Stopping Range of Ions and Matter (SRIM). Damage induced by H ions was much less than that by He ions while the concentration of H was a little larger than that of He. The peak depth of irradiation damage for both ions was approximately 280 nm.

### 2.3. TEM observation and nanoindentation test

Microstructures after ion irradiation were observed by FEI F-20 High Resolution Transmission Electron Microscopy (HRTEM). To evaluate irradiation hardening caused by different microstructural evolution, nanoindentation test was performed by Nano Indenter XP at RT. A diamond Berkovich tip with a radius of 20 nm was used with CSM method. The indentation depth was 1000 nm and nine indents were chosen for each sample with a space larger than 50 µm.

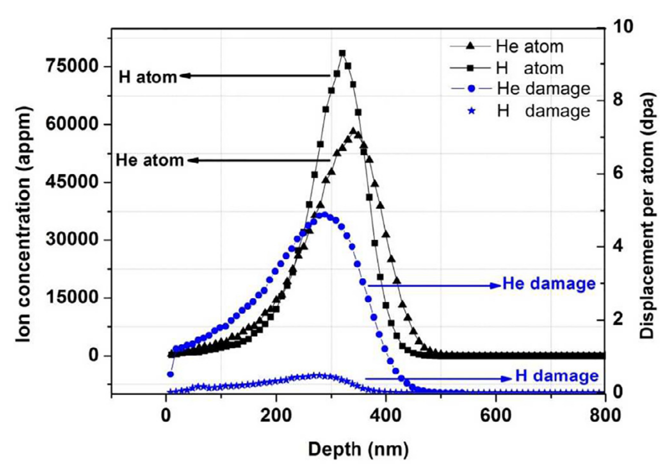


**Fig. 1.** Depth profile of atoms distribution and damage events for He$^{+}$irradiation and H$^{+}$irradiation.

## 3. Results and discussion

### 3.1. Microstructure after ion irradiation

Microstructure of V-4Cr-4Ti after different irradiation condition is shown in Fig. 2. The typical point defects were observed in Fig. 2a and b after He and He + H ions irradiation at RT in V-4Cr-4Ti alloys. Point defects include vacancy and interstitial produced during irradiation. These point defects have very small size and high number density. From TEM image, we cannot distinguish them one by one. Despite the fact that He damage is higher than H damage which indicated in Fig. 1, there is no obvious microstructural difference regardless of He or He + H irradiation at RT in V-4Cr-4Ti alloys. HRTEM images showed severe lattice distortion which was caused by defects in primary collision and cascade collision of irradiated ion and recoil ions [16]. In addition, no obvious bubble was visible in V-4Cr-4Ti alloys after He and He + H ion irradiations at RT.

After He and He + H ions irradiation at 300 °C, dislocation loops and bubbles were dominant in V-4Cr-4Ti alloys shown in Fig. 2c and d. The size and number density of dislocation loops was 25 nm and $5.4 \times 10^{10}$/cm$^2$ after He ions irradiation at 300 °C (Fig. 2c) and for He + H ions irradiation at 300 °C it was 8 nm and $3.6 \times 10^{11}$/cm$^2$ (Fig. 2d). The size of bubbles was 7 nm after He ions irradiation and 9 nm after He + H ions irradiation at 300 °C. The number density of bubbles were not estimated due to uncertainty.

The main reason for different microstrucutes between RT and 300 °C was temperature. At higher temperature point defects begin to migrate. The migration of interstitials is faster than vacancies which is involved in the strong formation of dislocation loops. According to other study, dislocation loops in this study are supposed to interstitial loops [17]. The migration energy of interstitial loops is very small [18]. The high mobility of interstitial loops at higher temperature promotes recombination with defects clusters or annihilation at other sinks [19].

The nucleation and growth of bubbles depend on He diffusion [2]. When irradiated He into materials, several combinations formed such as He clusters and He-vancacy complexes. The movement of He clusters and He-vancacy complexes was limited at RT. Temperature increment increases the rate of He diffusion. The subsequent H irradiation also produces point defects. However, the ability of helium binding cluster is much stronger than that of H. Therefore, these point defects continue to be absorbed by pre-formed He clusters and He-vancacies complexes [20]. H might be trapped by clusters and promote the nucleation of bubble [21]. For this reason, bubbles formed after He and H irradiation at 300 °C were He bubbles which had some H.

### 3.2. Irradiation hardening

To evaluate irradiation hardening caused by different microstructural evolutions, nanoindentation test was performed by Nano Indenter XP at RT. As shown in Fig. 3a, irradiation hardness versus the depth in irradiated V-4Cr-4Ti alloys under different irradiation conditions. Irradiation hardness was described by representative curves with different colors which meaned different irradiation conditions. Hardness values decreased with increasing indent depth over 50 nm while increased from surface to about 50 nm which were noticed as indentation size effect (ISE) and reverse ISE [22], respectively.

The curves of average nanoindentation hardness with error bar as a function of depth for four series of samples under different irradiation conditions are indicated in Fig. 3b. The hardness first decreases rapidly and then becomes flat as the depth increases for all the samples. The ISE can be excluded by Nix-Gao model [23] as follows: